

This is a copy of the published version, or version of record, available on the publisher's website. This version does not track changes, errata, or withdrawals on the publisher's site.

Preliminary lab demonstration of a 3-sided reflective pyramid wavefront sensor for Shane AO using SEAL testbed

Dominic Sanchez, Philip Hinz, Mark Chun, Christopher Ratliff, Daren Dillon, et al.

Published version information:

Citation: DF Sanchez et al. Preliminary lab demonstration of a 3-sided reflective pyramid wavefront sensor for Shane AO using SEAL testbed. Proc SPIE 12185 (2022):121858F. Is in proceedings of: Adaptive Optics Systems VIII, Montréal, Québec, Canada, 17-23 Jul 2022

DOI: [10.1117/12.2630724](https://doi.org/10.1117/12.2630724)

Copyright 2022 Society of Photo-Optical Instrumentation Engineers (SPIE). One print or electronic copy may be made for personal use only. Systematic reproduction and distribution, duplication of any material in this publication for a fee or for commercial purposes, and modification of the contents of the publication are prohibited.

This version is made available in accordance with publisher policies. Please cite only the published version using the reference above. This is the citation assigned by the publisher at the time of issuing the APV. Please check the publisher's website for any updates.

This item was retrieved from **ePubs**, the Open Access archive of the Science and Technology Facilities Council, UK. Please contact epublications@stfc.ac.uk or go to <http://epubs.stfc.ac.uk/> for further information and policies.

PROCEEDINGS OF SPIE

[SPIDigitalLibrary.org/conference-proceedings-of-spie](https://spiedigitallibrary.org/conference-proceedings-of-spie)

Preliminary lab demonstration of a 3-sided reflective pyramid wavefront sensor for Shane AO using SEAL testbed

Dominic Sanchez, Philip Hinz, Mark Chun, Christopher Ratliff, Daren Dillon, et al.

Dominic F. Sanchez, Philip M. Hinz, Mark Chun, Christopher Ratliff, Daren Dillon, Charlotte Z. Bond, "Preliminary lab demonstration of a 3-sided reflective pyramid wavefront sensor for Shane AO using SEAL testbed," Proc. SPIE 12185, Adaptive Optics Systems VIII, 121858F (29 August 2022); doi: 10.1117/12.2630724

SPIE.

Event: SPIE Astronomical Telescopes + Instrumentation, 2022, Montréal, Québec, Canada

Preliminary lab demonstration of a 3-sided reflective pyramid wavefront sensor for Shane AO using SEAL testbed

Dominic F. Sanchez^a, Philip M. Hinz^a, Mark Chun^b, Christopher Ratliff^a, Daren Dillon^a, and Charlotte Z. Bond^c

^aUniversity of California Santa Cruz, 1156 High St, Santa Cruz, CA 95064

^bInstitute for Astronomy, University of Hawaii, 34 Ohia Ku St, Makawao, HI 96768

^cThe UK Astronomy Technology Centre, Royal Observatory Edinburgh, Edinburgh, UK

ABSTRACT

In this paper, we present the preliminary results for a three-sided reflective pyramid wavefront sensor (3-RPWFS) for Shane Telescope's adaptive optics module. HCIPy simulations using a modulation radius of $5\lambda/D$ indicate comparable performance to the module's existing Shack-Hartmann wavefront sensor. An opto-mechanical design is modeled to meet the physical constraints for Shane AO installation and future on-sky testing. A closed-loop demonstration of a 3-RPWFS prototype is conducted using the SEAL testbed, and it yields promising results illustrating proof of concept. We discuss the details of the simulation, opto-mechanical design, and SEAL closed-loop results for the 3-RPWFS.

Keywords: pyramid wavefront sensing, reflective pyramid, adaptive optics, three sided pyramid

1. INTRODUCTION

Direct imaging is a powerful method in characterizing exoplanets because it angularly resolves the planet and allows us to disentangle planet and host star light. In order to reach this level of resolution, extremely large telescopes (ELTs) are under development to meet this technological need. Although telescope size, and observation wavelength, determine the theoretical angular resolution, the wavefront aberrations caused by light propagating through the atmosphere is the main limitation for ground-based telescopes. Adaptive optics (AO) allows us to restore some of this lost resolution by measuring these distortions and applying corrections with compensating optical elements. A key component of these future telescope AO systems will be a highly sensitive wavefront sensor (WFS) – such as the pyramid wavefront sensor (PWFS).¹

Traditional PWFSs utilize a four-sided glass prism; light from the telescope focuses onto the pyramid apex and produces four pupil images. Like that of the Foucault knife-edge test, the light distribution between the pupils in this sensor holds information about the optical aberrations in the system. Unfortunately, fabricating these glass prisms is difficult due to its geometry and leads to optical imperfections.² A three-sided pyramidal prism, on the other hand, is easier to fabricate and reduces the impact of these imperfections. Studies indicate that a three-sided PWFS (3-PWFS) may be less sensitive to read noise because it requires fewer pixels for wavefront sensing. In both transmissive designs, chromatic aberrations are inherent; wavelength dependent refractive indices give rise to optical aberrations and decreases the optical performance.

In this paper, we present a preliminary demonstration of a three-sided reflective pyramid wavefront sensor (3-RPWFS) using the Santa Cruz Extreme Adaptive Optics Laboratory (SEAL). A simulation, using the High-Contrast Imaging python package (HCIPy), is used to assess its performance using the Shane Telescope on Mount Hamilton and its results are described in Sec. 2. The proposed opto-mechanical design for on-sky testing on the Shane Telescope is briefly described in Sec. 3. Using SEAL, the initial closed-loop results of this 3-RPWFS is described in Sec. 4, and a discussion of the results are concluded in Sec.5.

Further author information: (Send correspondence to Dominic F. Sanchez)
E-mail: dfsanche@ucsc.edu

2. HCIPY SIMULATION

In this section, we review the simulated results for a 3-RPWFS in the Shane Telescope's AO module. These simulations were done using HCIPy and are meant to mimic and assess the performance of the proposed WFS. These simulations will be used to determine the 3-RPWFS design parameters for future on-sky testing with the Shane Telescope. For each simulation, the Strehl ratio (S) is used as the performance metric with a 1 sec exposure.

2.1 Assumptions

We use the specifications of the Shane AO module as the input parameters for the following 3-RPWFS simulations. A table of these relevant parameters are shown in Table 1. A multi-layered atmosphere with scintillation using Fried parameters (r_0) values of 7.5 cm and 11 cm are used.

Table 1. HCIPy Simulation Parameters.

Science Wavelength (λ_{obs})	2.2 μm
WFS Wavelength (λ_{WFS})	750 nm
Telescope Diameter (D_T)	3 m
Fried Parameter (r_0)	7.5 cm, 11 cm
Transmission (T)	50%
Quantum Efficiency (QE)	0.8
Read Noise (N_r)	5.1 e-
Number of DM actuators (n_{act})	121 (11x11)
Modulation Steps (n_{steps})	18
Number of AO Time Steps (t_{steps})	200

2.2 Modulation Radius

Under large turbulence or optical aberrations, the beam focusing onto the pyramid is modulated around the apex to increase its linear dynamic range and the optimal modulation radius (r_{mod}) is dependent on the amount of these distortions. The trade-off between sensitivity and linear dynamic range for the PWFS precludes a single modulation radius for all conditions; therefore, a simulation of the AO performance as a function of r_{mod} is performed. The simulated atmosphere uses a 1.5 arcsecond seeing for a conservative assessment with the 3-RPWFS.

The results of the simulations are shown in Fig. 1. There seems to be a small trend where the WFS performance peaks between $3-7\lambda/D$. The trade-off between sensitivity and dynamic range explains the drop-off in performance outside of this interval; smaller r_{mod} allows for higher sensitivity with a decrease in linear range and the opposite is true for a sensor with larger r_{mod} . In an attempt to optimize sensitivity while maintaining performance in non-ideal seeing conditions, we propose using a $r_{mod} = 5 \lambda/D$ for testing on the Shane Telescope.

2.3 Limiting Guide Star Magnitude

The current Shane AO module utilizes a Shack-Hartmann wavefront sensor (SH-WFS) which can achieve a $S = 0.6$ using a guide star magnitude (M_a) of 10. For comparison, the performance of the proposed 3-RPWFS is simulated to determine the limiting guide star magnitude for wavefront correction. The astronomical seeing is assumed to be 1-arcseconds, and corresponds to good seeing conditions. The modeled 3-RPWFS is simulated with $r_{mod} = 5 \lambda/D$. The simulation results, as shown in Fig.2 indicate similar performance to that of the SH-WFS with $M_a = 10$, and with $S \geq 0.4$ for $M_a \leq 11$ at 500 Hz. At 100 Hz, the 3-RPWFS reaches a peak $S = 0.51$, and maintains $S \geq 0.2$ for $M_a \leq 13$, increasing the limit by approximately over a magnitude. Strehl ratios below 0.2 are not considered accurate because they cannot be approximated well analytically. With these results, the 3-RPWFS is expected to have comparable performance to the existing SH-WFS, and can use guide stars as dim as $M_a \approx 13$ at 100 Hz.

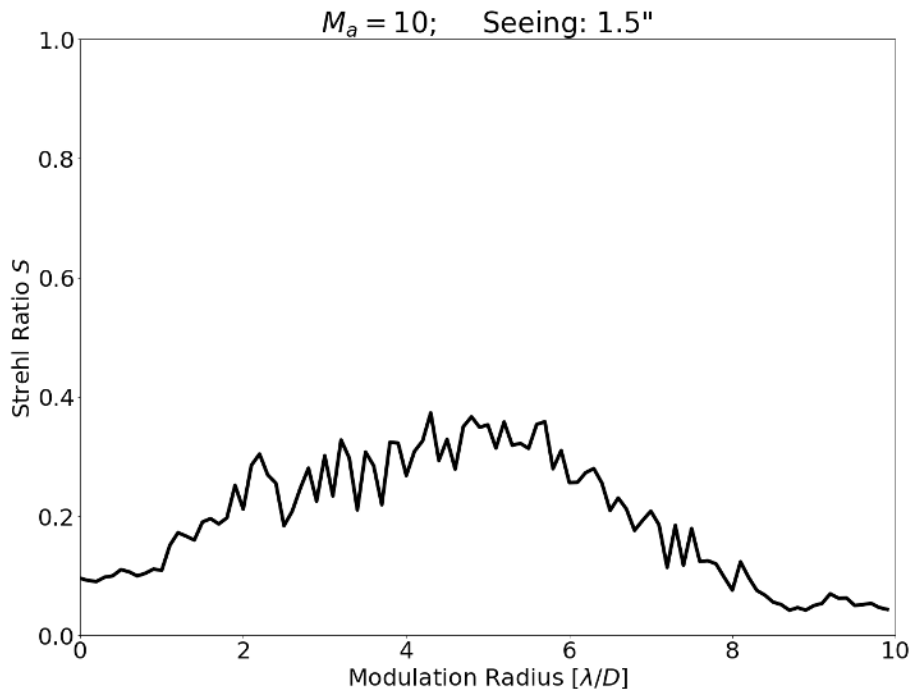


Figure 1. A plot showing the Strehl ratio as a function of modulation radius for the 3-RPWFS.

3. OPTO-MECHANICAL DESIGN

In the following sections, we briefly describe the opto-mechanical design for the 3-RPWFS and its optical configuration for the Shane AO module. The optical design is discussed in more detail in Ref. 3, but a brief overview is given in the following section.

3.1 Optical Configuration

Typically, PWFSs require light from the telescope to be focused onto the pyramid apex. In the traditional transmissive designs, this focusing beam propagates through the glass prism and produces four pupil images behind the pyramid for wavefront measurement. The focusing beam is usually modulated using a fast-steering mirror; this increases the linear range of the WFS under large aberrations but decreases its sensitivity.

Unlike the transmissive design, the beam focusing onto the pyramid apex cannot propagate through the prism in a RPWFS. There are multiple optical configurations for a fully reflective PWFS; however, the Shane AO module constrains our RPWFS to one on-axis WFS detector for wavefront measurement.

The proposed Shane AO 3-RPWFS optical configuration is shown in Fig. 3. The incoming F/21.08 telecentric focusing beam is re-focused using a triplet lens, which produces an F/50 focusing beam onto the apex. Instead of a mirror, this F/50 beam is modulated using a spinning glass wedge located at the reimaged pupil location. After reflecting from the apex, the three beams are reimaged behind the prism using a parabolic mirror that collimates the light. Three through-holes are drilled into the reflective pyramid to allow the collimated pupil images behind the pyramidal prism. Lastly, three radially separated doublet lenses reimage each pupil image onto the detector.

3.2 Mechanical Design

The existing Shane AO module has an optical tube assembly (OTA) with a SH-WFS, which is positioned inside a v-groove mount. The current mechanical design allows for translation and rotation along the z-axis. The v-block mount and OTAs are shown in Fig. 4.⁴ This mechanical configuration is the motivation behind the 3-RPWFS optical design; the Shane AO module and OTA does not easily allow for a fully reflective system.

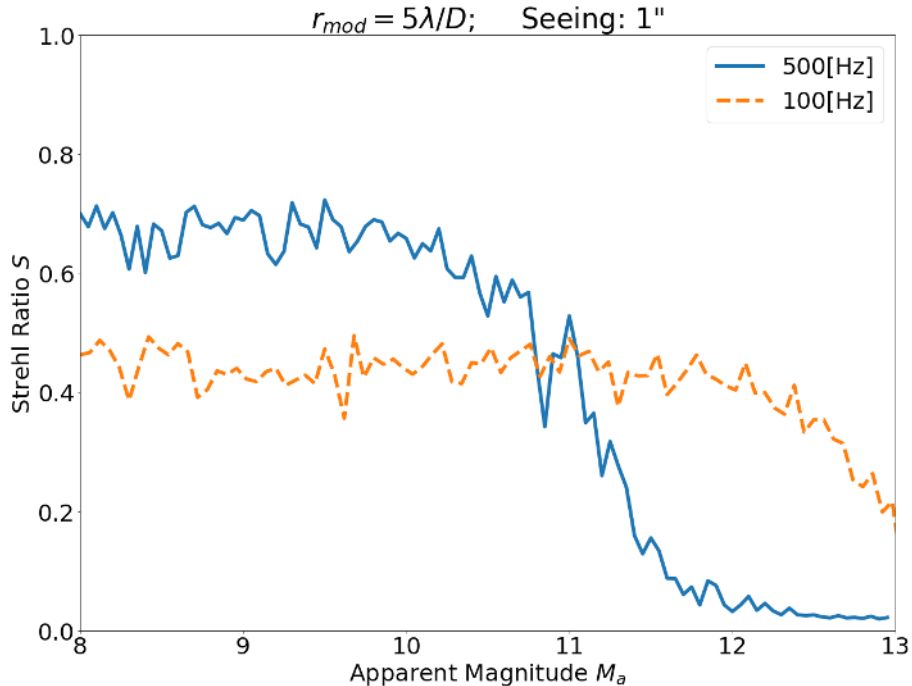


Figure 2. Plot showing the Strehl ratio as a function of guide star magnitude while running the AO system at two different frequencies.

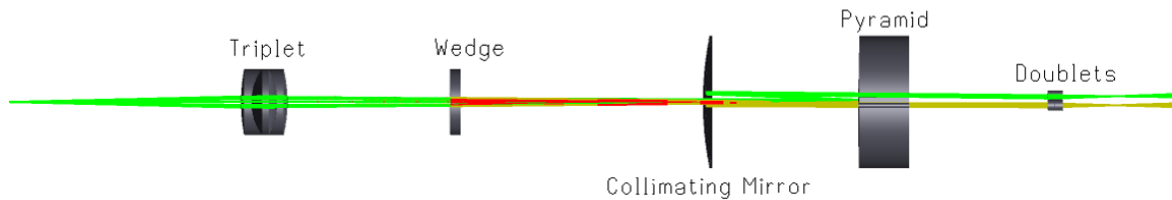


Figure 3. Zemax OpticStudio model of the 3-RPWFS designed for Shane AO. The three wedge configurations are organized by color and they show the expected ray path while modulating the beam.

The Shane AO module will be retrofitted with the 3-RPWFS, and therefore its mechanical design will also use an OTA to ease implementation. A cross-sectional view is shown in Fig. 5. The key differences to note will be the beam alignment after collimation and the beam modulator. The pyramid and the three doublets can be independently translated and rotated, which allows for the three reflected collimated beams to be aligned. Due to the optical power of the three doublet lenses, their lens mount will have tip, tilt, and X-Y translation capability to minimize aberrations from misalignment.

The glass wedge must be spun along the optical axis to produce a circular modulation pattern. We want to operate at frequencies up to 500 Hz, and the exposure time must match this frequency to evenly distribute light within a modulation cycle. This is done using a friction drive, where a BLDC motor spins a mounted Viton O-ring and its contact with the wedge mount drives the wedge to spin by friction. The modulator's mechanical design is shown in Fig. 6 and it is controlled using a Raspberry PI 3B. The maximum rate the modulator has been tested is ~ 450 Hz. This compact device allows us to install the 3-RPWFS and continue using the existing v-groove stage.

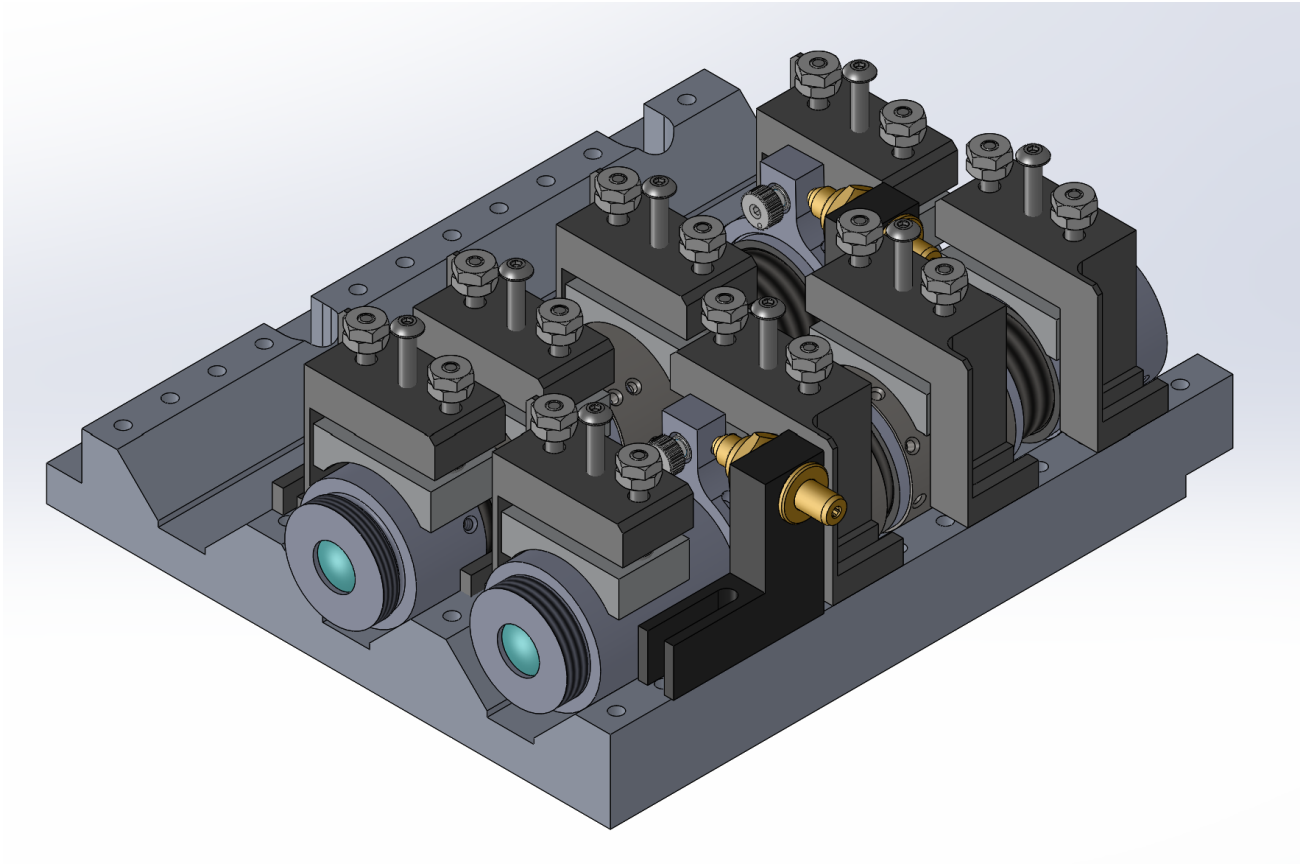


Figure 4. SolidWorks model of the existing Shane AO module. The OTAs, from left to right, are the 16x and 8x SH-WFS options for wavefront measurement. These assemblies are positioned inside a v-groove and the assembly can be translated in plane perpendicular to the optical axis. The proposed 3-RPWFS OTA will be installed in the farthest left open v-groove track.

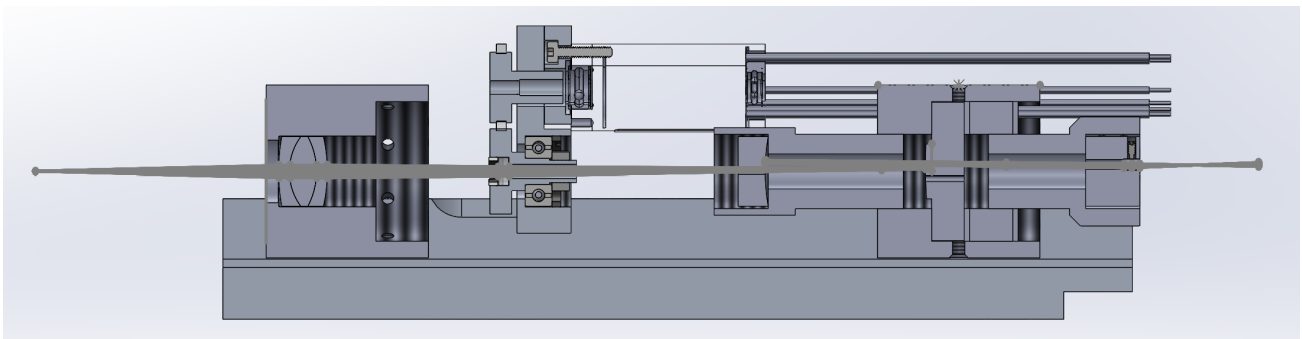


Figure 5. A cross-section view of the proposed 3-RPWFS opto-mechanical design for Shane AO testing.

4. SEAL DEMONSTRATION

4.1 Optical Setup

An in-lab demonstration of a 3-RPWFS is performed using SEAL. The optical outline of the 3-RPWFS in this testbed is shown in Fig. 7. We use a ALPAO deformable mirror (DM) with a 13.5 mm circular aperture and 97 actuators – 11 actuators across the pupil. After beamsplitting the light, a pair of relay lenses minimize the beam, and two additional optical elements are introduced to simulate the F/21.08 telecentric beam in the Shane

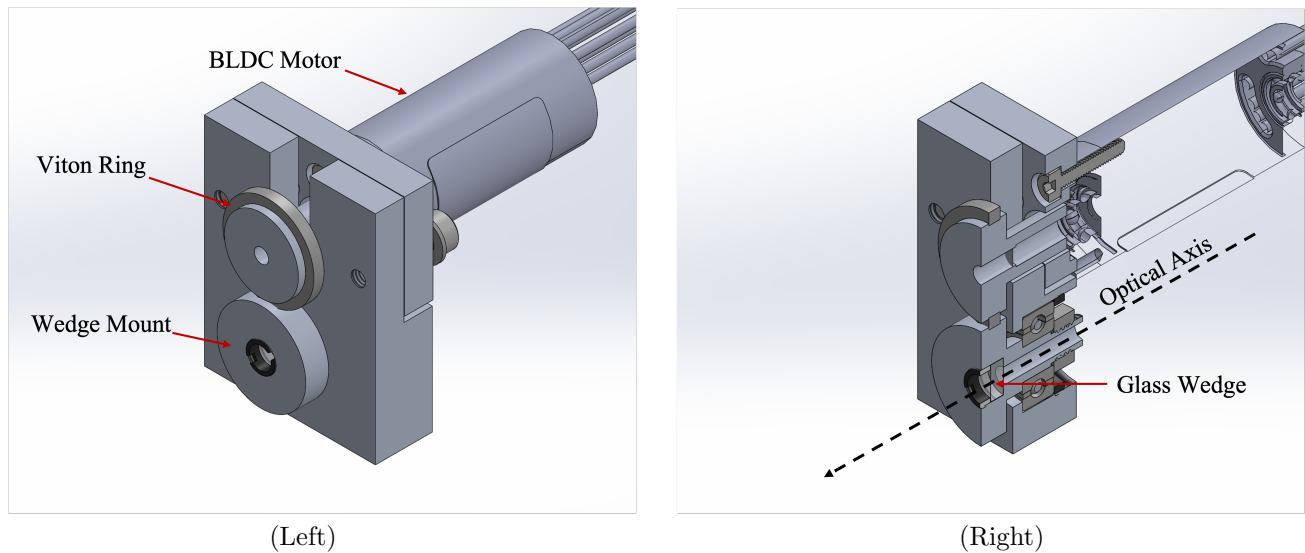


Figure 6. (Left) Model of the beam modulator assembly. A Viton O-ring around a disk is attached to the motor shaft. The O-ring makes contact with the wedge mount, which holds the modulating wedge. (Right) A cross-section view showing the glass wedge and the optical axis.

AO module. Fig. 8 shows the 3-RPWFS optical setup used for the SEAL demonstration. The OTA assembly described in Sec.3 has not yet been implemented; therefore, an analogous system is tested instead. The final pupil signals from the 3-RPWFS are imaged using three radially separated doublet lenses. However, in this lab demonstration, these images will instead be relayed using two 100 mm focal length lenses. Furthermore, we use a 1920x1200 FLIR Blackfly detector with 5.86 μm pixels. The main goal is to demonstrate the feasibility of the 3-RPWFS device by demonstrating closed loop operation.

4.2 Calibration

We began our calibration by first flattening the DM using the SH-WFS in SEAL, which converged to approximately 50 nm rms. The modal interaction matrix is then constructed by measuring the actuator influence using a poke matrix; each DM actuator is poked and the resulting flattened pupil images were collected into a matrix. The Moore-Penrose pseudoinverse is calculated for the poke matrix and Zernike modal basis of 100 modes is used to create the interaction matrix. The reference pupil images are subtracted to measure the phase response from each poked actuator. A plot comparing the simulated HCIPy and SEAL 3-RPWFS pupil images are shown in Fig. 9. Each row represents, from top to bottom, the applied DM shape, the simulated pupil images using HCIPy, and the RPWFS pupil images collected in SEAL respectively. There are geometrical differences between the simulated and SEAL pupil images because there are additional upstream optical elements that change the pupil geometry within the clear aperture. The footprint of another DM is seen in the reference pupil images in SEAL, which is not modeled in HCIPy.

4.3 Closing the Loop

The modulating frequency is set to 100 Hz and the exposure time is set for a 8 modulation cycles per exposure. Modulating frequency is set and measured using a Raspberry PI 3B. The controller uses a leaky integrator, with a leakage and gain value of 0.01 and 0.5 respectively. Fig. 10 shows the resulting point spread function (PSF) from these applied DM shapes in the top row, and the resulting corrected PSF after 50 AO correction steps in the bottom row.

Qualitatively, the RPWFS effectively measures the induced aberrations for wavefront corrections. For example, the PSF has the classical radial spread associated with defocus – the same behavior is seen with the higher order spherical aberration. When applying Z_1^{-1} , the PSF is expected to translate within the image plane; however, we notice additional induced higher order modes (See Z_1^{-1} , middle row).

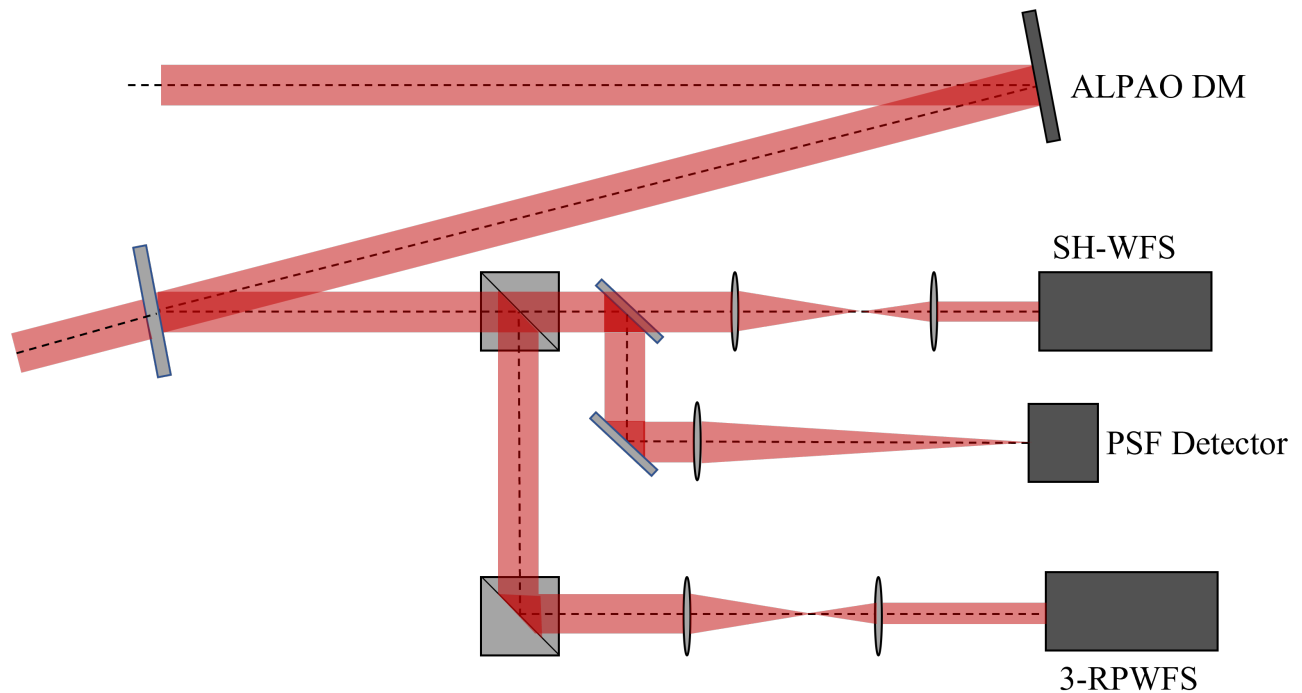


Figure 7. 3-RPWFS SEAL layout used for lab demonstration. Additional optical elements were installed to mimic a F/21.08 telecentric beam before entering the 3-RPWFS.

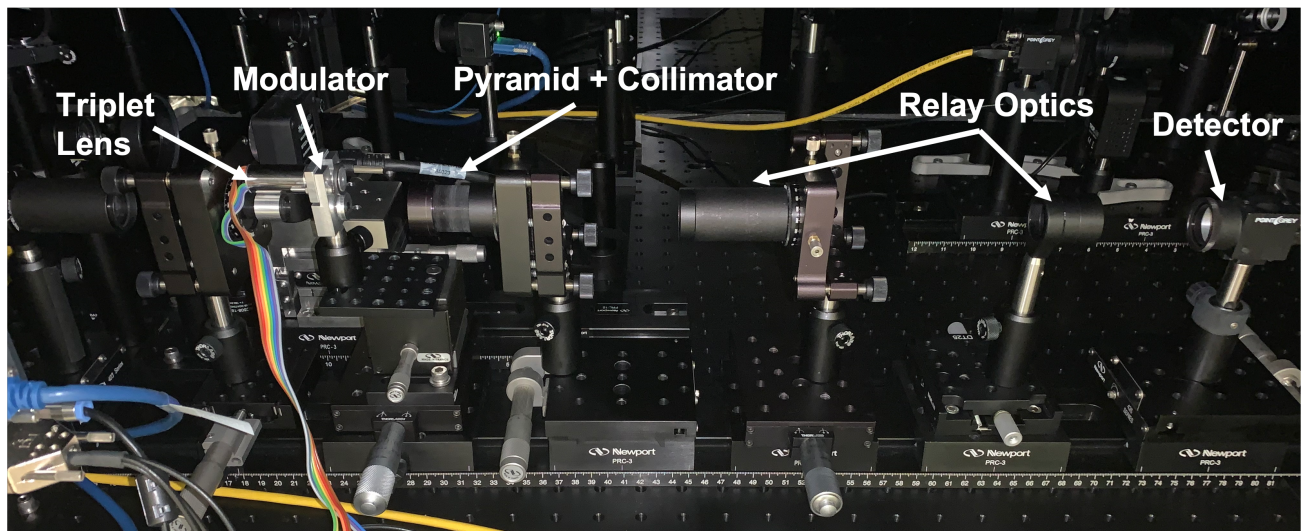


Figure 8. Lab setup for the SEAL 3-RPWFS demonstration. One-to-one conjugate relay lenses are used to reimagine the pupils onto the detector.

5. DISCUSSION AND CONCLUDING REMARKS

In this paper, we simulated, designed, and lab tested a 3-RPWFS for the Shane AO module. At the time of writing this paper, the mechanical are being fabricated to better simulate the proposed 3-RPWFS assembly. This in-lab 3-RPWFS prototype yields promising preliminary results for on-sky feasibility.

The 3-RPWFS is conservatively simulated to determine optimal r_{mod} for wavefront sensing on the Shane

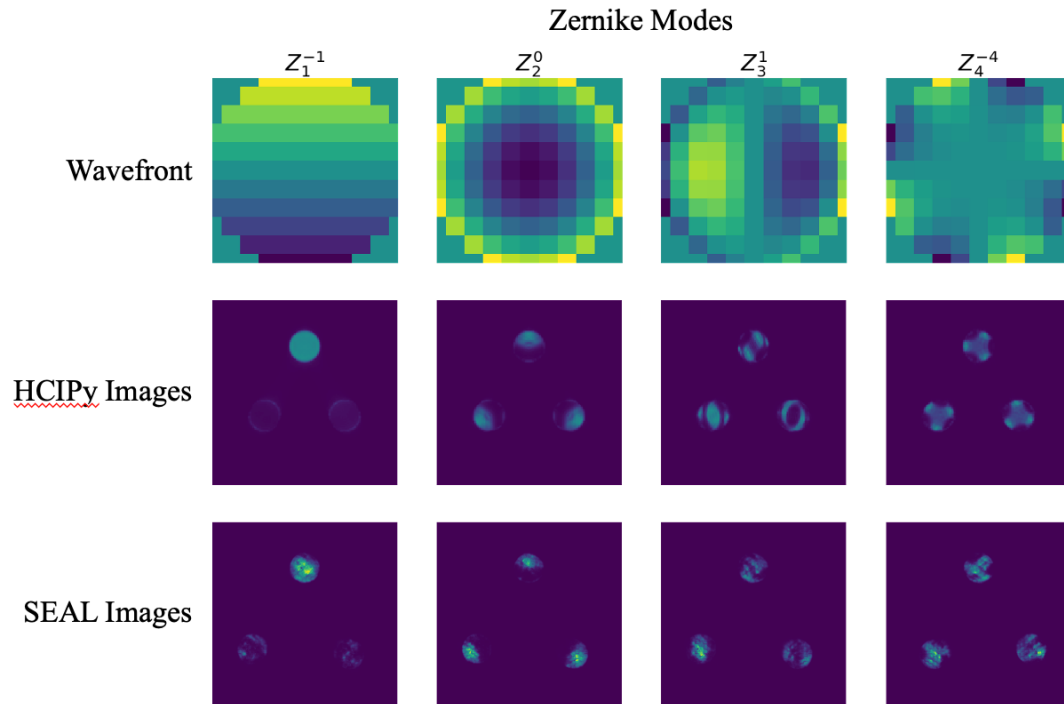


Figure 9. (Top) The wavefront applied to the ALPAO DM after flattening. (Middle) The expected 3-RPWFS pupil images simulated using HCIPy. (Bottom) The pupil images collected using SEAL testbed. An $80\ \mu\text{m}$ P-V is applied for each Zernike mode.

Telescope. Without sacrificing too much sensitivity or linear dynamic range, we use a $r_{mod} = 5\ \lambda/D$ for initial testing. These simulations indicate that this sensor is capable of meeting current SH-WFS Strehl ratios, and under good seeing conditions with $r_{mod} = 5\lambda/D$, the 3-RPWFS can achieve $S \geq 0.2$ for $M_a \leq 13$. Although these results are encouraging, a more thorough analysis of the modulated PWFS simulations is needed to build a more conclusive performance ceiling. The modulation steps and pupil grid sampling used to model the PWFS seems to impact the reference pupil images; a coarse pupil grid resolution leads to unequal light distribution between the pupil images with small r_{mod} and fewer n_{steps} . These issues can be mitigated using higher resolution grids and more n_{steps} ; however, increasing n_{steps} leads to lengthy simulation run times.

The opto-mechanical 3-RPWFS prototype is designed as a retrofit for the Shane AO module for on-sky testing. The tight opto-mechanical constraints limit the device configuration to the one described in Ref.3. With this in mind, the glass wedge is modulated using a compact friction drive where a BLDC motor spins the wedge through friction using contact with a Viton O-ring. This assembly is capable of spinning up to 1 kHz and produces a circular modulation pattern in the image plane. Not yet tested in the SEAL testbed, the reimaging doublet lenses will have additional degrees-of-freedom for alignment and limit static aberrations. The optical system is designed to be diffraction limited within 500-900 nm.

A closed-loop lab demonstration is conducted using SEAL and a modal interaction matrix is calibrated using 100 Zernike modes. The 3-RPWFS is able to create aberrated pupil images that are generally consistent the HCIPy simulations. Because the testbed also has three upstream DMs, the pupil image geometry differs from those in seen in the HCIPy simulations. There are other differences, which are more easily seen with a Z_1^{-1} DM shape. We expect to see a PSF translation vertically along the science image plane; however, additional higher order modes are being induced along with Z_1^{-1} – as seen by the blurred PSF. This discrepancy may stem from an insufficient reference DM flat, non-common path aberrations, and/or an incorrect assumption of the applied DM shape.

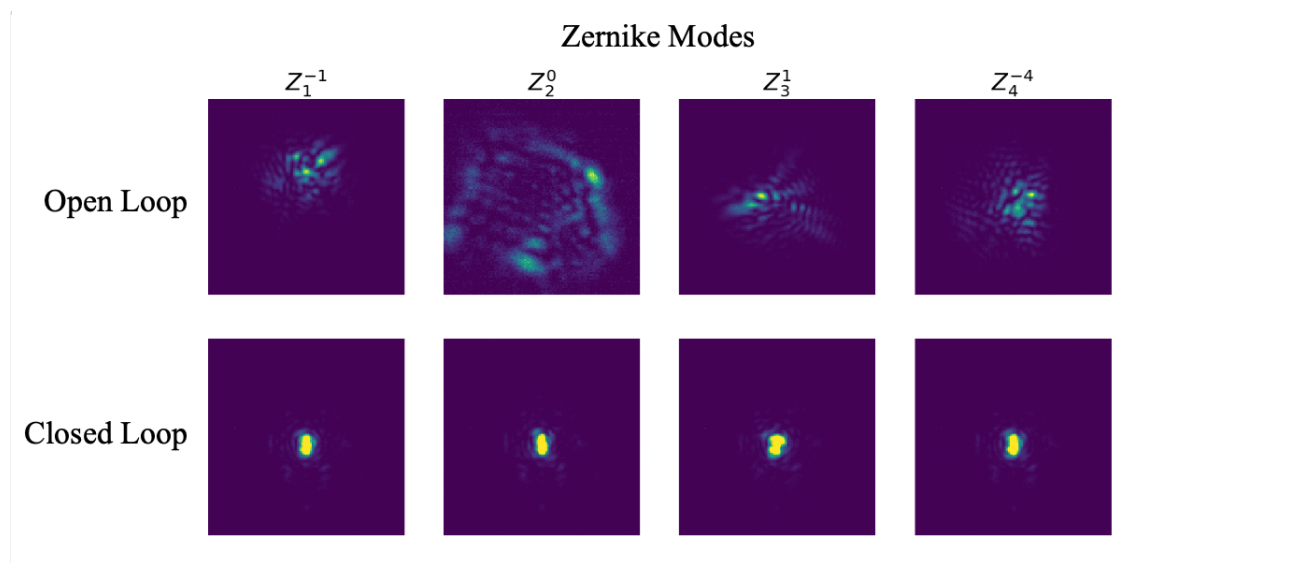


Figure 10. (Top) The PSF images for each Zernike mode before closed loop correction. (Bottom) The resulting PSFs after closed loop correction.

Before installing the 3-RPWFS for on-sky testing, the proposed opto-mechanical design must be assembled and analyzed using SEAL for a more conclusive assessment of the device. The in-lab experiments described in this paper operated at a low frequency (100 Hz) and the 3-RPWFS has yet to be tested at its expected peak frequency of 1 kHz. In all, these initial 3-RPWFS lab results are promising and a more quantitative analysis will be conducted for a more conclusive demonstration.

ACKNOWLEDGMENTS

We thank the University of California Santa Cruz for funding this research. We also thank Reni Kupke, Rebecca Jensen-Clem, Benjamin L. Gerard, Maaike Van Kooten, Rachel Bowens-Rubin, and Jules Fowler for their discussions on the project. D.F. Sanchez acknowledges support from the Eugene Cota-Robles Fellowship.

REFERENCES

- [1] Ragazzoni, R., “Pupil plane wavefront sensing with an oscillating prism,” *Journal of Modern Optics* **43**, 289–293 (Feb. 1996).
- [2] Fauvarque, O., Neichel, B., Fusco, T., Sauvage, J.-F., and Girault, O., “General formalism for Fourier-based wave front sensing: application to the pyramid wave front sensors,” *Journal of Astronomical Telescopes, Instruments, and Systems* **3**, 019001 (Jan. 2017).
- [3] Sanchez, D. F., Chun, M., Bond, C. Z., and Hinz, P. M., “Design study for a three-sided reflective pyramid wavefront sensor for Shane AO,” in [*Adaptive Optics Systems VII*], Schreiber, L., Schmidt, D., and Vernet, E., eds., **11448**, 753 – 762, International Society for Optics and Photonics, SPIE (2020).
- [4] Ratliff, C., Cabak, J., Gavel, D., Kupke, R., Dillon, D., Gates, E., Deich, W., Ward, J., Cowley, D., Pfister, T., and Saylor, M., “Opto-mechanical design of ShaneAO: the adaptive optics system for the 3-meter Shane Telescope,” in [*Adaptive Optics Systems IV*], Marchetti, E., Close, L. M., and Véran, J.-P., eds., **9148**, 1135 – 1148, International Society for Optics and Photonics, SPIE (2014).